Asian Journal of Chemistry; Vol. 34, No. 12 (2022), 3215-3223

ASIAN JOURNAL OF CHEMISTRY

https://doi.org/10.14233/ajchem.2022.23977

# Synthesis of Ternary CaNiAl-Layered Double Hydroxide as Potential Adsorbent for Congo Red Dye Removal in Aqueous Solution

DEEPMONI BRAHMA, KASTURI PRIYOM NATH, MADHUSMITA PATGIRI and HEMAPROBHA SAIKIA*

Department of Chemistry, Bodoland University, Kokrajhar-783370, India

*Corresponding author: E-mail: saikiahemaprobha@gmail.com

*Received*: 21 June 2022; *Accepted*: 30 September 2022; *Published online*: 25 November 2022; AJC-21047

A hierarchically porous ternary CaNiAl-LDH material was synthesized *via* a facile urea hydrolysis method and characterized by PXRD, FT-IR, BET, SEM and TGA techniques. The adsorption efficiency of synthesized ternary CaNiAl-layered double hydroxide was also examined using Congo red dye as a model pollutant. Material characteristics affirmed with the formation of circular and flower-like LDH particles with accessible mesopores of 3.85 nm and intermediate surface area of 58.45 $m^2$/g. The synthesized ternary CaNiAl-LDH material exhibited the maximum adsorption capacity of 135.21 mg/g towards the targeted organic pollutant from an aqueous medium. The obtained results in isotherm and kinetic studies demonstrated that sorption of Congo red dye onto CaNiAl-LDH followed Langmuir isotherm and pseudo-second order model, respectively. In addition, the thermodynamic studies also suggested the endothermic and spontaneity of the sorption process. The reusability studies confirmed that CaNiAl-LDH can be reused up to fourth cycle. Therefore, the proposed material CaNiAl-LDH can be advocated as a highly effective low cost adsorbent for the treatment of water contaminants.

**Keywords: Layered double hydroxide, Congo red dye, Adsorption, Intercalation.**

## INTRODUCTION

With the fast growth of urbanization, the discharge of effluents from various manufacturing industries had created environmental hazard for all living species due to its diverse effect. Among several water pollutants, the use of synthetic azo dyes had emerged rapidly due to its wide applications in industries such as textile, plastic, leather, foods, cosmetics, medicine and paper [1]. Dyes disperse in water bodies leads to coloured water, which can block the radiation from sunlight and can affect aquatic life forms. In addition, azo dyes have complex and stable chemical structure that makes it very difficult to separate or degrade from the water bodies *via* conventional methods [2]. Due to its recognized carcinogenic and mutagenic effects, it is also extremely poisonous and causes variations in parameters like BOD and COD levels, which can be harmful for all types of habitat. In particular, Congo red (CR) dye a type of azo dye is highlighted toxic and causes adverse effects such as irritation, cancer, photosynthesis inhibition, reduction in oxygen level and suffocating flora and fauna [3]. Therefore, it is imperative to treat azo dye-polluted wastewaters in order to reduce the pollutants present in the industrial effluents.

For wastewater treatment, a number of techniques and methods are developed in order to reduce the adverse affects of poisonous dyes. Some widely used efficient techniques that can achieve dye separation from an aqueous medium are filtration [4], coagulation/flocculation [5], ozonation [6], photodegradation [7] and adsorption [8]. However, adsorption method is deemed as one of the most preferred approach in remediation of various toxins from liquid phase. Due to ease of operation, low cost, high efficiency, non-toxic and mild reaction condition, it can be easily afforded. This technique can be applied to separate, purify, detoxify and deordorize the toxic product in both liquid and gaseous medium. A large number of adsorbents were reported for the removal of Congo red dye, for instances Metal-organic frameworks (MOFs) [9], activated carbon [10], polymer composite [11], zeolite [12] and LDH [13]. Moreover, due to its multiple advantages, such as flexible structure, high surface area, thermal stability, ease of regeneration and non-toxicity, layered double hydroxide (LDH) can be considered one of the most promising candidates in water pollution treatment.

Layered double hydroxides (LDHs) are the broad class of anionic clays, which is generally represented by the chemical formula $[M^{2+}_{1-x}M^{3+}_{x}(OH_2)]^{x+}(A^{n-})_{x/n}\cdot H_2O$ where $M^{2+}$ ($Ca^{2+}$, $Mg^{2+}$, $Fe^{2+}$, $Ni^{2+}$), $M^{3+}$($Fe^{3+}$, $Al^{3+}$, $Cr^{3+}$) and $A^{n-}$($CO_3^{2-}$, $Cl^-$, $NO_3^-$) are divalent metal cation, trivalent metal cations and interlayer ions, respectively. Designing of LDH can be achieved through various synthetic routes such as hydrothermal, urea hydrolysis, co-precipitation, rehydration/construction, ion exchange. In addition, anion exchange in the structure can be tuned by intercalating with various organic and inorganic ions, which plays a key role in the adsorption process [14,15]. Consequently, to improve the sorption characteristics of binary LDH, the variation in the structure can be made by introducing third metal ions.

In this work, an attempt is made to synthesize ternary CaNiAl-LDH *via* urea hydrolysis method. The as-synthesized sorbents were implemented for the removal of targeted azo-dye (Congo red dye) from the aqueous solution. The influence of the adsorption parameters such as pH, temperature, dosages, contact time, initial dye concentration on the adsorption performances was investigated. The reusability studies are also conducted. The isotherm and kinetic studies were also reported and the plausible mechanism of dye sorption were also analyzed by recording P-XRD and FT-IR spectra of the sample after adsorption of Congo red dye.

## EXPERIMENTAL

Nickel chloride hexahydrate ($NiCl_2\cdot 6H_2O$), calcium chloride dihydrate ($CaCl_2\cdot 2H_2O$), aluminium chloride, sodium hydroxide were procured from Merck, while urea and Congo red dye ($C_{32}H_{22}N_6O_6S_2Na_2$) were purchased from Qualigens India Pvt. Ltd. All the obtained chemicals were of analytical grade and utilized directly without any further purifications.

**Preparation of adsorbents:** Layered double hydroxide (LDH) sample was prepared *via* a facile urea hydrolysis method. Initially, a mixture of metal precursor's solutions containing 8 mmol $NiCl_2\cdot 6H_2O$, 8 mmol $CaCl_2\cdot H_2O$ and 4 mmol $AlCl_3$ in a 100 mL aqueous solution was stirred. Subsequently, 2.1 g of urea was further added to the above solution mixture and continuously stirred until the precursors were completely dissolved. The resulting suspension was then transferred in autoclave and heated at 150 ºC in an oven for 6 h. The obtained green precipitate was collected and washed several times with deionized water. Finally, the resulting product was dried in a vacuum at 50 ºC and crushed with mortar to obtain the powder form, which is denoted as CaNiAl-LDH.

**Adsorption experiments:** To investigate the adsorption efficiency of ternary CaNiAl-LDH, the adsorption isotherm experiment was conducted in a batch mode. In isotherm studies, a stock solution of Congo red dye having initial concentration from 30 to 270 mg/L was prepared in distilled water. A Congo red dye solution (20 mL) at varying initial concentration was taken in a conical flask and 0.025 g of adsorbent was mixed. The resulting solution was then allowed to stir at 28 ºC (room temperature) in a water bath shaker for time period of 6 h to attain equilibrium. The adsorbent was separated from the liquid suspension by filtration and the concentration of Congo red dye in filtrate was measured by using UV-Spectrophotometer at the absorption maximum wavelength of 498 nm. The percentage removal and quantity of Congo red dye adsorbed on to CaNiAl-LDH was calculated by the given equation:

$$\text{Dye removal } (\%) = \frac{C_o - C_e}{C_o} \times 100 \quad (1)$$

$$q_e = \frac{(C_o - C_e)V}{W} \quad (2)$$

where $C_o$ and $C_e$ denotes initial and equilibrium dye concentration, respectively; $q_e$ indicates amount of dye adsorbed at equilibrium, V represents volume of the adsorbate solution (mL) and W signifies the quantity of adsorbent (g).

In kinetic studies, 0.025 g of adsorbent CaNiAl-LDH was mixed with 40 mL of Congo red dye solution at the initial dye concentration (50 mg/L). The liquid suspension is then allowed to agitate in a shaker for a time period of 3 h. After a definite time interval, 2 mL of the solution was withdrawn and separated from the adsorbent by centrifugation at 1000 rpm. Similarly, the residual dye concentration was estimated at the maximum absorption wavelength of 498 nm. The quantity of dye uptake at time 't' was evaluated by the equation:

$$q_t = \frac{(C_o - C_t)V}{W} \quad (3)$$

where $q_t$ represents amount of dye adsorbed at time 't', $C_t$ indicates the concentration of dye at time 't'.

## RESULTS AND DISCUSSION

**XRD studies:** The PXRD spectra of the synthesized hierarchically porous ternary CaNiAl-LDH before and after sorption of Congo red dye are shown in Fig. 1. The characteristics pattern of the typical layered double hydroxide structure was exhibited in pristine CaNiAl-LDH. The peaks observed at 2θ values 11.34º, 22.94º, 34.88º, 39.17º, 46.48º, 60.75º, 62.17º were attributed to corresponding indexed plane 003, 006, 009, 015, 018, 110, 113, respectively [16]. A well-crystalline character of the as-synthesised sample is further supported by a strong reflection in the XRD spectrum. However, the evaluated values of $a = 0.3$ nm and $c = 2.34$ nm based on expressions ($a = 2d_{110}$, $c = 3d_{003}$) were found almost constant for CaNiAl-LDH and CaNiAl-LDH-Congo red. Since, the shifting of peaks was not observed after the adsorption of Congo red dye, thus it can be anticipated that sorption takes place on the external surface rather than intercalation on the interlamellar spaces [17].

**FT-IR studies:** The identification of surface functionalities was performed by FT-IR analysis as shown in Fig. 2. The broad band at 3489 $cm^{-1}$ arises due to –OH stretching vibration of water molecule. Another band detected at 1641 $cm^{-1}$ is attributed to the bending vibration of –OH group. A sharp absorption peak at 1370 is assigned to the interlayer $NO_3^-$ ion and the low intensity band between 800-600 $cm^{-1}$ was noticed due to M-O stretching vibration (Ca-O, Al-O, Ni-O). After adsorption of Congo red molecule, the spectrum of CaNiAl-LDH-Congo red manifested two small new peaks at 1043 $cm^{-1}$ and

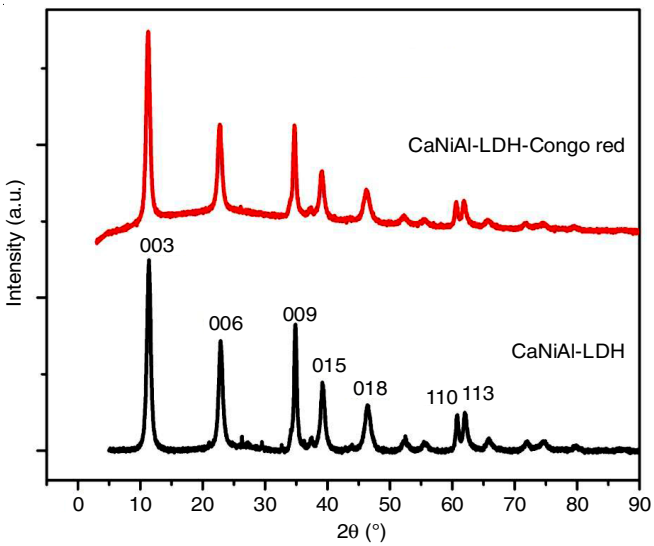


Fig. 1. P-XRD spectra of CaNiAl-LDH before and after adsorption of Congo red dye

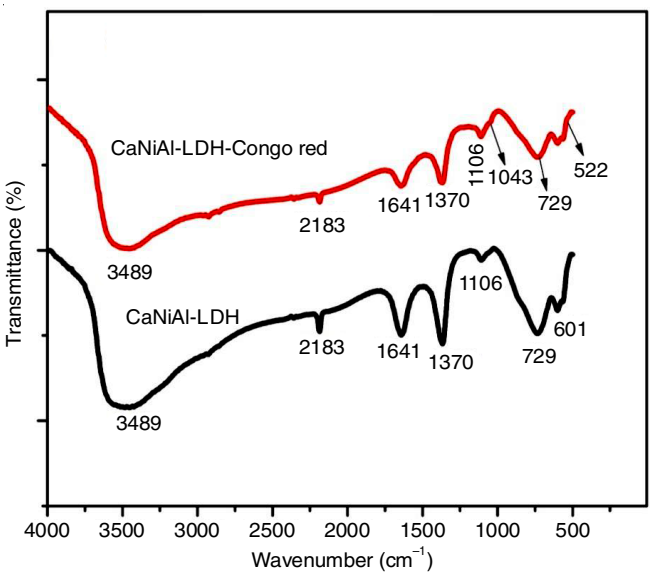


Fig. 2. FT-IR spectra of CaNiAl-LDH before and after adsorption of Congo red dye

522 $cm^{-1}$, which confirms that sorption of Congo red dye molecules over the surface of adsorbent occurred. In addition, the intensity of the peaks also reduced after adsorption in comparison to pristine CaNiAl-LDH. Thus, the result was consistent and strongly suggests the active role of surface functional groups during the adsorption of targeted pollutants [18,19].

**Adsorption-desorption isotherms:** Fig. 3 illustrates the $N_2$-adsorption desorption isotherms of ternary CaNiAl-LDH; while the insets of Fig. 3 showed the pore size distribution curve determined based on BJH method of the sample. The isotherm curve is consistent with type-IV isotherm and $H_3$-hysteresis loop, which signifies the presences of mesopores on the material. In Fig. 3, it is observed that the isotherm curve generates slowly at higher relative pressure ($P/P_o < 0.8$), which depicts the inter particle mesoporosity of CaNiAl-LDH. The specific surface area, pore size and pore volume of the as synthesized sample were 58.45 m/g, 3.85 nm and 0.106 cc/g, respectively [20].

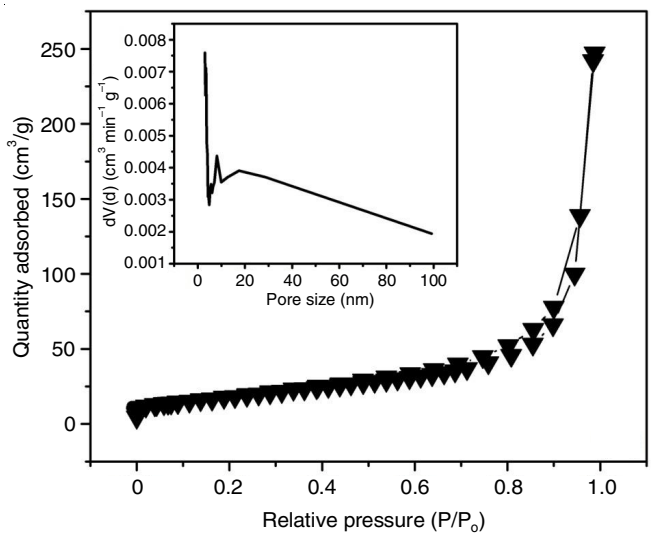


Fig. 3. $N_2$-adsorption desorption isotherm curve of CaNiAl-LDH

**Thermal studies:** The mass decomposition of the synthesized CaNiAl-LDH sample was studied by thermogravimetric analysis. The TGA curve (Fig. 4) shows that mass losses takes place at three different stages. The initial mass loss of 11.62% in the region between 30-220 ºC was observed due to the elimination of physio adsorbed water molecule. The highest mass loss of 19.07% takes place in the second step around (220-574 ºC), which can be ascribed to the removal of interlayer ions such as $NO_3^-$, $CO_3^{2-}$, $Cl^-$. Moreover, the final stage of mass loss (4.4%) arises between 574-721 ºC, where the layered structure of CaNiAl-LDH gets completely destructed and beyond 720 ºC, the curve appears to be a constant straight line without further mass loss [21].

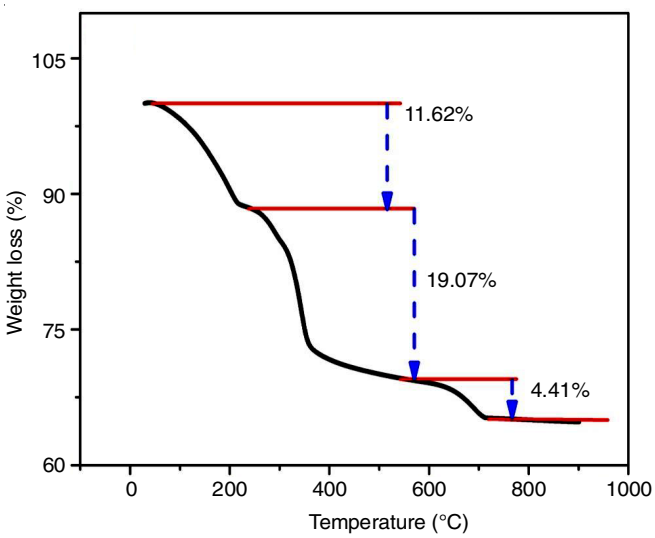


Fig. 4. TGA profile of the adsorbent CaNiAl-LDH

**Morphology studies:** The SEM images of pristine CaNiAl-LDH at different resolution (100 nm, 200 nm, 1 µm) are shown in Fig. 5. The synthesized hierarchically porous ternary LDH showed smooth structure with circular and flower petals like shape with an average size below 300 nm. The uniform distribution of the LDH particle over the adsorbent

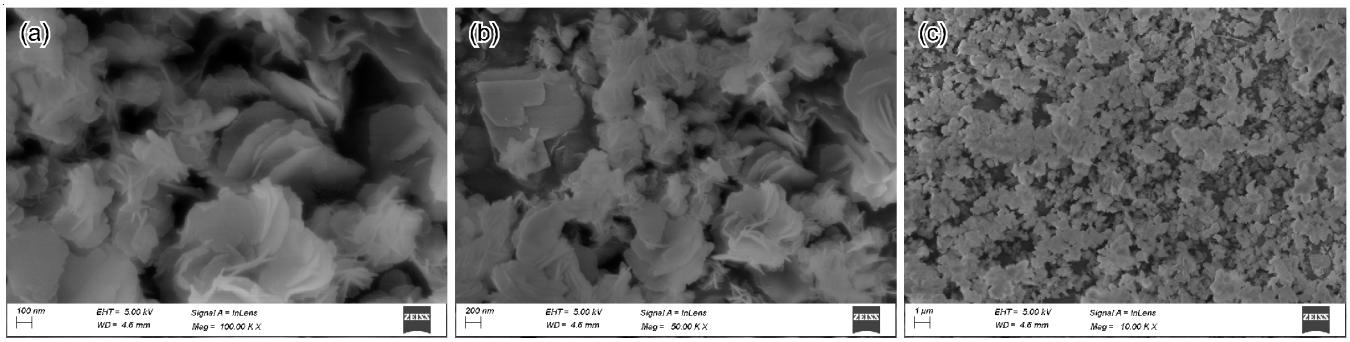


Fig. 5. SEM images of the adsorbent at different magnifications (10 K×, 50 K× and 100 K×)

surface can be ruled out (Fig. 5c), which also reflect the formation of characteristics LDH platelets with many pores existing in it, which could be responsible and contributes in the good adsorption performance of the material [22,23].

**Adsorption isotherm:** In isotherm studies the three most widely used models namely Langmuir [24], Freundlich [25] and Temkin [26] were employed for investigating the sorption behaviour of Congo red dye on to ternary CaNiAl-LDH. Based on Langmuir model, it assumes that adsorption of the solute molecules over the homogeneous surface takes place through the formation of monolayer, while the Freundlich model explains the adsorption process where development of multiple layer occurs in the heterogeneous surface. The non-linear expression for Langmuir, Freundlich and Temkin model are given as:

$$q_e = \frac{q_{max} C_e K_L}{1 + K_L C_e} \quad (4)$$

$$q_e = K_f C_e^{1/n} \quad (5)$$

$$q_e = B_T \ln(K_T C_e) \quad (6)$$

where $C_e$ (mg/g) is the equilibrium concentration of dye solution; $q_m$ is the maximum monolayer adsorption capacity, $K_L$ and $K_f$ are the Langmuir constant and Freundlich constant, respectively. The index 'n' indicates the intensity of adsorption; $B_T$ and $K_T$ are the Temkin constant, which signifies heat of adsorption and equilibrium binding constant.

Fig. 6 demonstrates the non-linear fitting of adsorption isotherms data for the sorption of Congo red dye molecules on to CaNiAl-LDH. The isotherm parameters are listed in Table-1. It is observed that the coefficient of determination for Langmuir ($R^2 = 0.972$) was found higher than other isotherm models such as Fruendlich ($R^2 = 0.850$) and Temkin ($R^2 = 0.926$). The maximum monolayer adsorption capacity ($q_{max}$ = 135.21 mg/g) value was evaluated from Langmuir model. The adsorption of Congo red dye on to CaNiAl-LDH was more suitable and can be best described according to Langmuir model, which shown

TABLE-1
ADSORPTION ISOTHERM PARAMETERS DETERMINED BY LANGMUIR, FREUNDLICH AND TEMKIN MODELS

| Isotherm model | Isotherm constant | Values |
|---|---|---|
| Langmuir | $q_{max}$ (mg/g) | 135.21 |
| | $K_l$ (L/mg) | 0.4543 |
| | $R^2$ | 0.972 |
| | $\chi^2$ | 44.62 |
| Freundlich | $K_f$ (mg/g)(L/mg)$^{1/n}$ | 55.59 |
| | n | 4.72 |
| | $R^2$ | 0.850 |
| | $\chi^2$ | 245.09 |
| Temkin | $B_T$ | 21.07 |
| | $K_T$ | 9.581 |
| | $R^2$ | 0.926 |
| | $\chi^2$ | 120.43 |

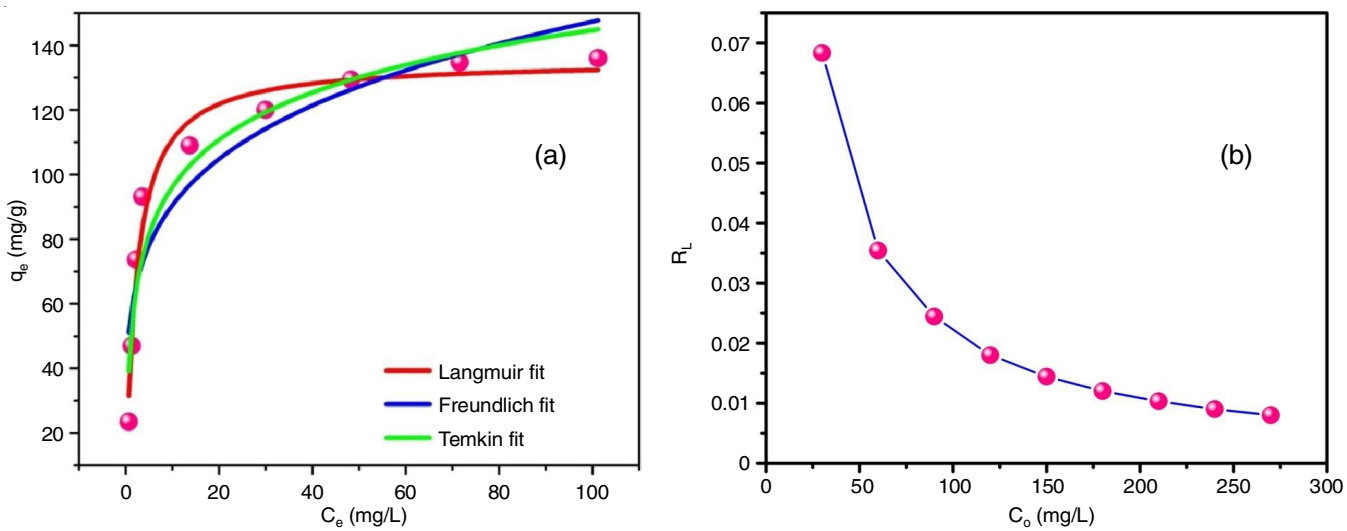


Fig. 6. (a) Non-linear adsorption isotherm curves based on Langmuir, Freundlich and Temkin models, (b) Graph of $R_L$ *vs.* $C_o$ plot

that adsorption was more likely to occur through single layer development.

The feasibility of the adsorption process was predicted by a separation factor ($R_L$), which can be estimated by the following equation:

$$R_L = \frac{1}{1 + K_L C_o} \quad (7)$$

The evaluated value of $R_L$ lies in the range of 0-1 for all initial dye concentration (30-270 mg/L). Thus, the obtained results indicated that adsorption was favourable [27].

**Adsorption kinetics:** To understand the adsorption rate of Congo red dye and the dynamics associated during the process, the kinetics studies was executed. The kinetic models applied for investigating Congo red dye adsorption on to the synthesized CaNiAl-LDH were pseudo-first order [28], pseudo-second order [29], intraparticle diffusion [30] and Elovich model [31]. The linearized equation for the respective models are given by:

$$\log(q_e - q_t) = \log q_e - \frac{K_1 t}{2.303} \quad (8)$$

$$\frac{1}{q_t} = \frac{1}{K_2 q_e^2} + \frac{t}{q_e} \quad (9)$$

$$q_t = K_i t^{0.5} + C \quad (10)$$

$$q_t = \frac{1}{\beta}\ln(\alpha\beta) + \frac{1}{\beta}\ln(t) \quad (11)$$

where $q_e$ is the quantity of dye adsorbed at equilibrium (mg $g^{-1}$); $q_t$ indicates the quantity of dye adsorbed at time t (mg $g^{-1}$); $K_i$ represents intraparticle diffusion constant and C is the boundary layer thickness.

The kinetics parameters for Congo red dye adsorption are summarized in Table-2. The best fitting of the kinetic model was determined by comparing the coefficient of determination ($R^2$) value. It is obvious that $R^2$ value (0.919) for pseudo-first order was lower than pseudo-second order (0.998), which indicates the more suitability of experimental data based on pseudo-second order model. The experimental $q_e$ (mg/g) value was also close to $q_{e2}$ (mg/g) than $q_{e1}$ (mg/g). Thus, the adsorption kinetics can be well explained with pseudo-second order model and thereby indicating the presences of chemisorptions [32].

TABLE-2
KINETIC PARAMETERS FOR THE ADSORPTION OF CONGO RED DYE ON To CaNiAl-LDH

| Kinetic model | Parameters | Values |
|---|---|---|
| Pseudo-first order | $q_{exp}$ | 38.396 |
| | $q_{e1}$ (mg/g) | 18.927 |
| | $K_1 \times 10^{-2}$ ($min^{-1}$) | 1.156106 |
| | $R^2$ | 0.919 |
| Pseudo-second order | $q_{e2}$ | 41.152 |
| | $K_2 \times 10^{-3}$ (g $mg^{-1}$ $min^{-1}$) | 1.072451 |
| | $R^2$ | 0.998 |
| Intraparticle diffusion | $K_i$ (mg/g $min^{-1}$) | 1.620 |
| | C (mg/g) | 15.245 |
| | $R^2$ | 0.774 |
| Elovich | β | 0.3215 |
| | α | 0.1284 |
| | $R^2$ | 0.923 |

Fig. 7c displayed the intraparticle diffusion plot ($q_t$ *vs.* $t^{0.5}$), which showed the presences of multiple stages during the sorption of Congo red dye molecules. The $q_t$ value between ($t_{0.5}$ = 0.385-0.833) increased quickly, while in the middle region bending of curves occurs due to diffusion into external pores. At the last stage, it tends to a constant straight line due to the achievement of equilibrium. Since, the plot of $q_t$ *vs.* $t^{0.5}$ did not pass through the origin, therefore the intraparticle diffusion is not the rate limiting step [33].

Similarly, based on Elovich model, the determined value of adsorption rate (α) and desorption rate (β) were found to be 0.128 and 0.321, respectively. The coefficient of determination value ($R^2$ = 0.923) also further suggests the applicability of this model [34].

**Effect of contact time:** The effect of contact time plays a key role in dye uptake. The removal efficiency of the adsorbate species as a function of contact time was investigated by fixing the experimental conditions with 50 mg/L initial concentration, 0.025 g dosages and contact time of 260 min, respectively. As shown in Fig. 8a, it is apparent that the adsorption rate occurs rapidly at the first 70 min where adsorption capacity ($q_t$) reaches up to 31.62 mg/g. This can be explained due to the easily available active site at the initial stage of contact time, which is followed by the steric repulsion of incoming Congo red dye molecules on the sorption site, thereby leading to the equilibrium stage after 175 min [35].

**Effect of adsorbent dosages:** Estimating the optimal dosages is critical for maintaining a cost-effective system. To investigate the effect of doses, the amount of adsorbent was varied from 0.005 g to 0.03 g at an initial dye concentration of 50 mg/L. The quantity of dye adsorbed ($q_e$) decreases from 170.16 to 32.44 mg/g and the removal percentage elevates from 85.08 to 97.34%. After 0.02 g dosages the removal efficiency does not increase significantly and remains constant (Fig. 8b). It is due to the fact that further increase in the applied adsorbent quantity may results in the accumulation of LDH particles which will not promote sorption of Congo red dye [36].

**Effect of initial dye concentration:** The effect of initial dye concentration is an important parameter and provides the essential driving force for adsorbing Congo red dye ions over the surface of adsorbents. Fig. 9a displayed the influence of initial dye concentration (30 to 270 mg/L) with 0.025 g dosages on the adsorption of Congo red dye molecules on to CaNiAl-LDH. Initially, high adsorption efficiency (97.77%) was observed at low adsorbate concentration due to the freely accessible sorption site, when the concentration of Congo red dye solution increases, the saturation on the adsorbent surfaces steadily decreases the removal efficiency [37].

**Effect of pH:** In present study, Congo red dye dye was selected as adsorbate and considering the effect of pH, the adsorption % were analyzed under pH 4, 7 and 10. The maximum removal % at pH 4, 7, 10 corresponding to the initial dye concentration (30 mg/L) were 97, 95.7 and 80%, respectively. Under acidic pH 4, the surface of CaNiAl-LDH bears the

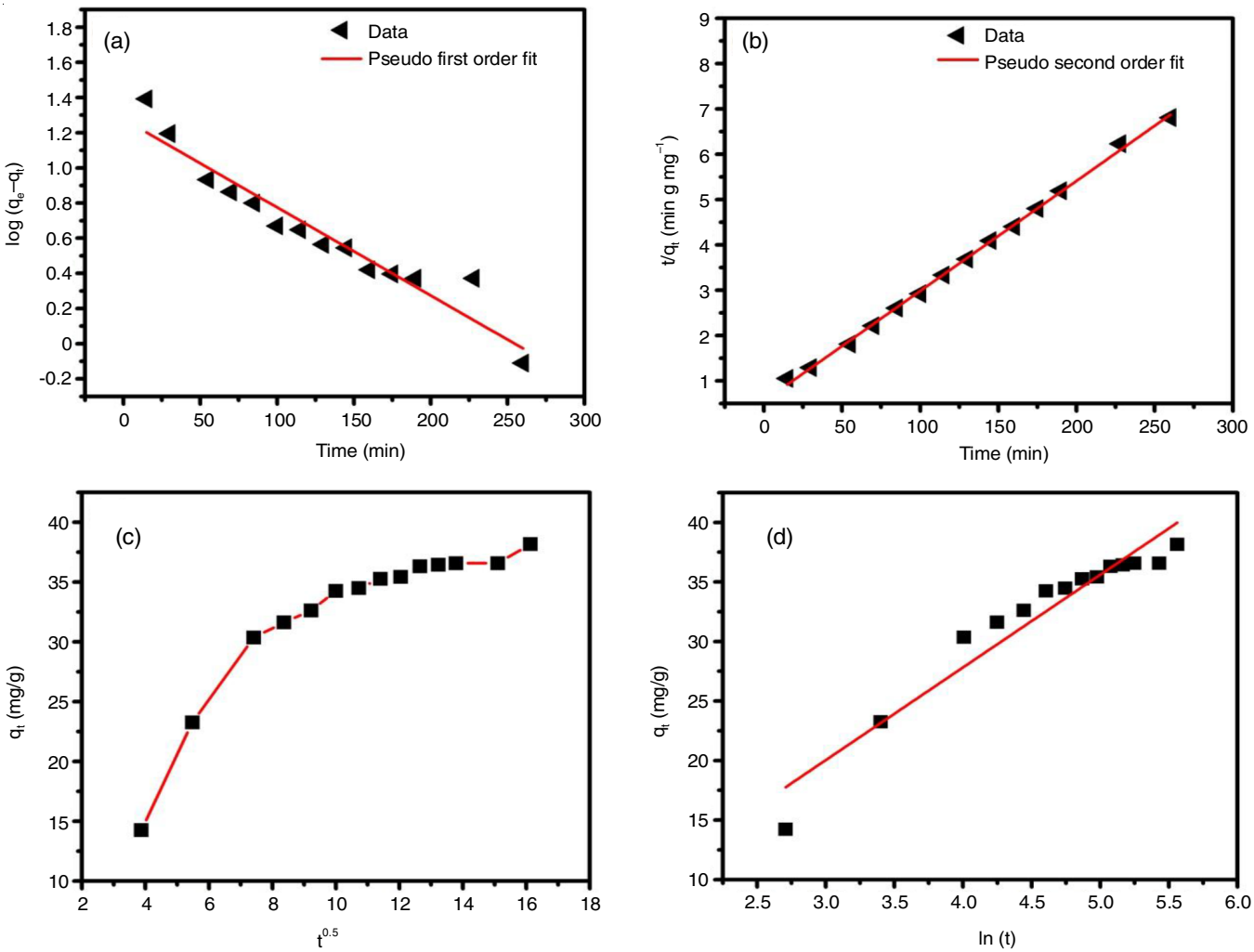


Fig. 7. Adsorption kinetic plots of Congo red sorption on to CaNiAl-LDH: (a) pseudo-first order, (b) pseudo-second order, (c) intraparticle diffusion and (d) Elovich plot

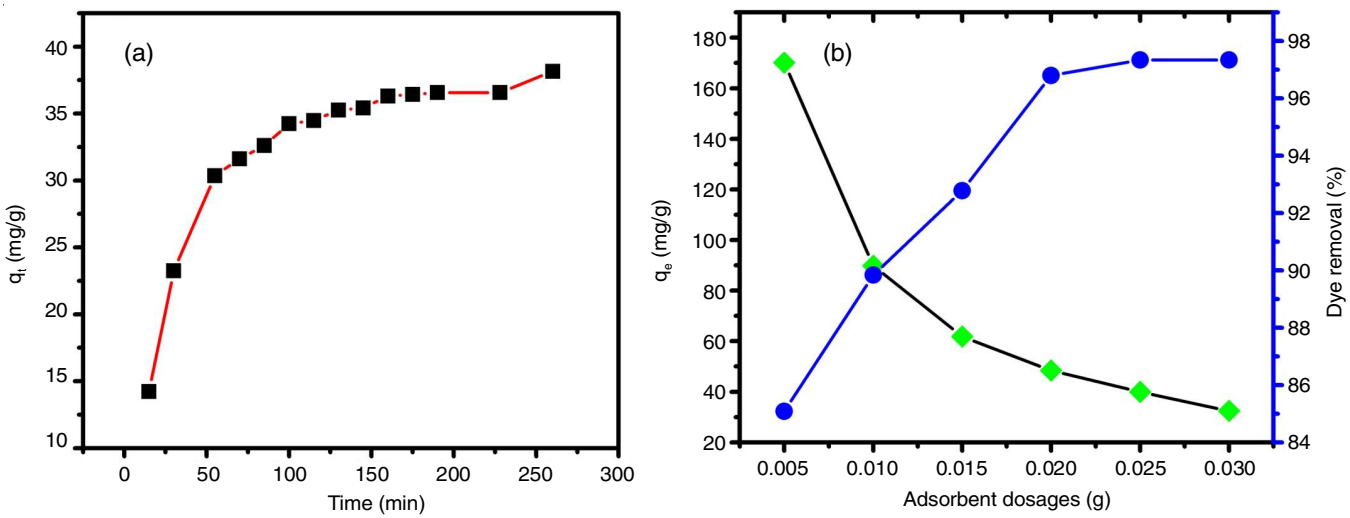


Fig. 8. Effect of contact time (a) and adsorbent dosages (b) on Congo red dye uptake by the adsorbent CaNiAl-LDH

additional positvie charge due to protonation ($H_3O^+$) from the solution (Fig. 9b). As a result, the electrostatic attraction between anionic Congo red dye ions and the positive charge LDH surfaces increases the sorption efficiency. On the contrary, at basic pH due to the the presences of competing negatively charged $OH^-$ ion, the adsorption of excess Congo red dye ions on the active site declines. Thus, the pH of the solution during the studies had shown notable effect [38].

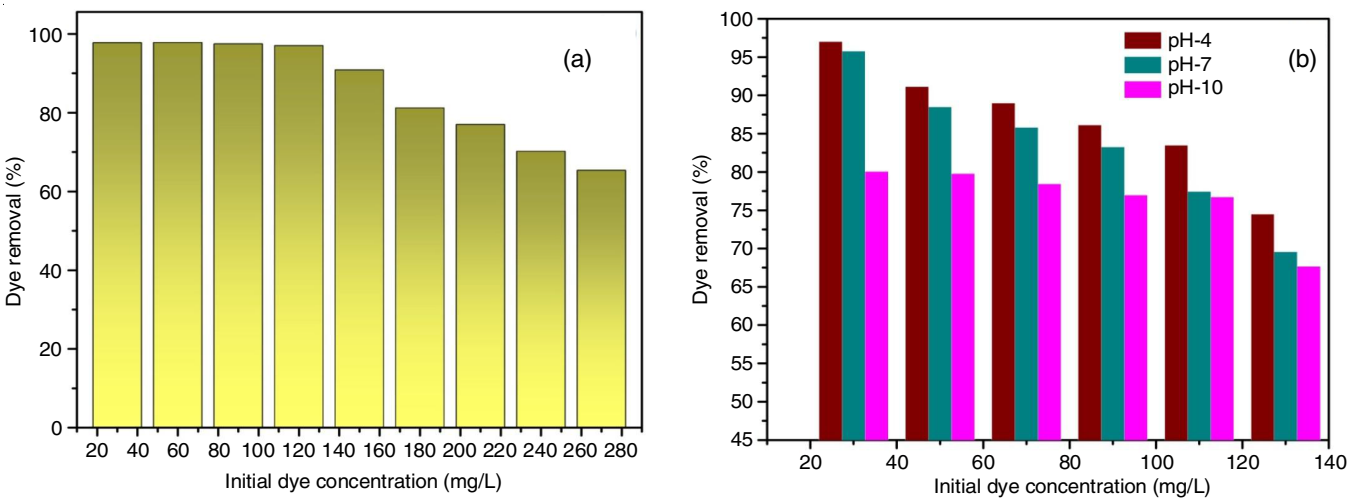


Fig. 9. Effect of initial concentration (a) and pH (b) on the percentage removal of Congo red dye

**Thermodynamic studies:** The thermodynamic studies were carried out for the adsorptive removal of Congo red dye ions at various temperature (30, 40, 50 ºC) using ternary CaNiAl-LDH adsorbents. The thermodynamic parameters such as Gibbs free energy (ΔG), enthalpy (ΔH) and entropy (ΔS) provide essential information regarding the feasibility of adsorption process. As a result, the estimation of these parameters was executed by using the following equations [39]:

$$\ln K_d = \frac{\Delta S}{R} - \frac{\Delta H}{RT} \quad (12)$$

$$\Delta G = -RT \ln K_d \quad (13)$$

where $K_d$ indicates adsorption distribution coefficient and R denotes the universal gas constant. The values of enthalpy change (ΔH) and entropy change (ΔS) was measured from the slope and intercept of the graph ln $K_d$ *vs.* 1/T ($K^{-1}$), respectively. The vant Hoff's plot was displayed in Fig. 10a and the obtained thermodynamic parameters are listed in Table-3. The negative value of ΔG implies that Congo red dye adsorption onto the CaNiAl-LDH was spontaneous and feasible process. As the temperature increased from 313 K to 333 K, ΔG value was found to decrease from -2.14 KJ/mol to -6.31 KJ/mol, thereby indicating the favourable adsorption process at higher temperature. However, the positive value of ΔH and ΔS, both demonstrated the endothermic nature of adsorption and increase in the randomness of the solid-liquid interfaces, respectively. The calculated ΔH value (63.10 KJ/mol) in the current research falls within the range for chemisorption processes, which typically have ΔH values between 80 and 200 KJ/mol. Therefore, it is hypothesized that the process of Congo red dye adsorption on CaNiAl-LDH will occur through physisorption [40].

**Comparison with reported adsorbents:** In previous report, various modified LDH listed in Table-4 showed the removal of Congo red dye from an aqueous solution. However, in recent studies, it is notable that the use of ternary CaNiAl-LDH exhibits greater adsorption capacity (135.21 mg/g) when compared to other adsorbents such as Mg-Fe-Al-LDH, MgAl-LDH, MNPs@NiFe-LDH and DS-Zn-Y hydroxide [41-48]. Therefore, the comparative result shows the feasibility of

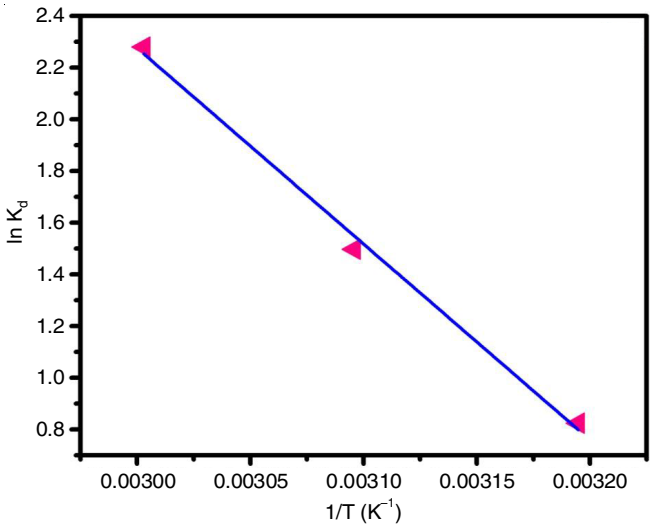


Fig. 10. vant-Hoff plot for estimation of various thermodynamic parameters in the sorption of Congo red dye

TABLE-3
CALCULATED THERMODYNAMIC PARAMETERS FOR THE CaNiAl-LDH-CR SYSTEM

| Adsorbent | +ΔH (KJ/mol) | +ΔS (J/mol) | -ΔG (KJ/mol) | | |
|---|---|---|---|---|---|
| | | | 313 K | 323 K | 333 K |
| CaNiAl-LDH | 63.038 | 208.032 | 2.14 | 4.02 | 6.31 |

TABLE-4
LIST OF REPORTED LDH BASED SORBENTS WITH THEIR $q_{max}$ VALUE FOR CONGO RED REMOVAL

| Adsorbents | $q_{max}$ (mg/g) | Ref. |
|---|---|---|
| MgAl-LDH | 111.11 | [40] |
| LDH-EDTA-AM | 632.9 | [41] |
| Mg-Fe-Al-LDH | 11 | [42] |
| ZnAl-LDH | 571.43 | [43] |
| Mg-Fe-$CO_3$-LDH | 104.6 | [44] |
| MNPs@NiFe-LDH | 79.6 | [45] |
| β-$Ni(OH)_2$/γ-$Fe_2O_3$/NiFe-LDH | 98.6-142.4 | [46] |
| DS-Zn-Y hydroxide | 96.24 | [47] |
| MgAl-LDH/γ-AlO(OH)/C | 447 | [48] |
| CaNiAl-LDH | 135.21 | This work |

CaNiAl-LDH as an effective adsorbent in Congo red dye removal.

**Reusability:** To determine the potentiality of the proposed adsorbents on industrial applications, the reusability test in the adsorption process was examined. For good adsorbents, the repeated use does not significantly decline its affinity towards targeted contaminants. In present studies, the reusability test was investigated up to fifth cycle. Fig. 11 revealed that the removal efficiency decreases from 95.73% to 75.99% as the recycle proceeds from first to last cycle. However, it is observed that the high sorption % of adsorbate molecules up to 75.99% was maintained even after fifth cycle, which shows its excellent performance for Congo red dye sorption. The slight decrease in removal percentage after successive use might be attributed to the loss of active site during regeneration.

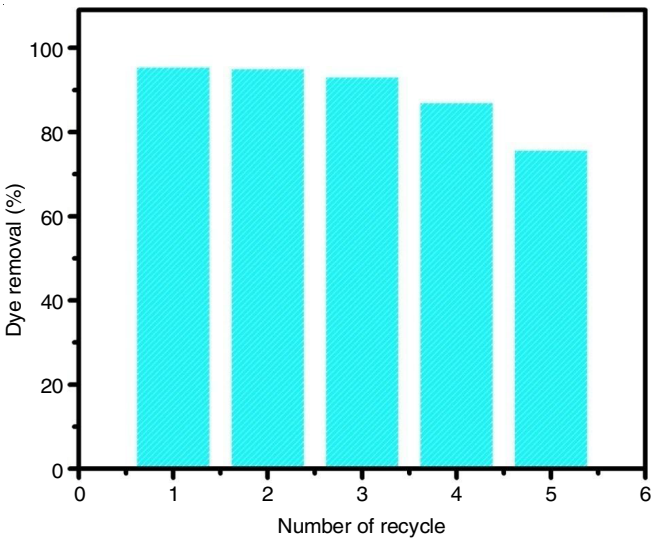


Fig. 11. Reusability efficiency of ternary CaNiAl-LDH in the removal of Congo red dye from an aqueous solution

## Conclusion

In summary, a ternary CaNiAl-LDH was synthesized by urea hydrolysis method and applied for the treatment of aqueous solution by selecting Congo red dye as a targeted pollutant. The unique physico-chemical properties of the proposed adsorbent CaNiAl-LDH such as porosity, high surface area and flower shaped LDH particles have contributed for the enhance sorption of Congo red dye. Moreover, the isotherm and kinetics data fitted well according to the Langmuir and pseudo-second order kinetic models. In addition, the main factor responsible for the adsorption of Congo red dye is due to the electrostatic attraction between the positively charged brucite sheets of LDH and negatively charged Congo red dye molcules. Thus, the present study sheds light in exploring ternary LDH and suggest that CaNiAl-LDH can be use as an alternative adsorbent for the treatment of dye contaminated wastewater.

## ACKNOWLEDGEMENTS

The authors are thankful to several institutes for providing instrumental facility for characterization of material with SEM, BET and powder X-ray from CIF, IIT Guwahati, FT-IR from Cotton University and thermogravimetric analysis from North East Hill University. Shillong, India

## CONFLICT OF INTEREST

The authors declare that there is no conflict of interests regarding the publication of this article.

## REFERENCES

1. W.-W. Li, H.-Q. Yu and B.E. Rittmann, *Nature*, **528**, 29 (2015); https://doi.org/10.1038/528029a
2. D. Iark, A.J.R. Buzzo, J.A.A. Garcia, V.G. Côrrea, C.V. Helm, R.C.G. Corrêa, R.A. Peralta, R.F. Peralta Muniz Moreira, A. Bracht and R.M. Peralta, *Bioresour. Technol.*, **289**, 121655 (2019); https://doi.org/10.1016/j.biortech.2019.121655
3. S.S. Yang, J.H. Kang, T.R. Xie, D.F. Xing, N.Q. Ren, S.H. Ho and W.M. Wu, *J. Clean. Prod.*, **227**, 33 (2019); https://doi.org/10.1016/j.jclepro.2019.04.005
4. A.B. Fradj, A. Boubakri, A. Hafiane and S.B. Hamouda, *Results in Chemistry*, **2**, 100017 (2020); https://doi.org/10.1016/j.rechem.2019.100017
5. C.Y. Teh, P.M. Budiman, K.P.Y. Shak and T.Y. Wu, *Ind. Eng. Chem. Res.*, **55**, 4363 (2016); https://doi.org/10.1021/acs.iecr.5b04703
6. S. Venkatesh, K. Venkatesh and A.R. Quaff, *J. Appl. Res. Technol.*, **15**, 340 (2017); https://doi.org/10.1016/j.jart.2017.02.006
7. S.Y. Lee, D. Kang, S. Jeong, H.T. Do and J.H. Kim, *ACS Omega*, **5**, 4233 (2020); https://doi.org/10.1021/acsomega.9b04127
8. A.K. Badawi, M. Abd Elkodous and G.A.M. Ali, *RSC Adv.*, **11**, 36528 (2021); https://doi.org/10.1039/D1RA06892J
9. Y. Tanimoto and S.I. Noro, *RSC Adv.*, **11**, 23707 (2021); https://doi.org/10.1039/D1RA03348D
10. R.A. El-Ghany Mansour, M.G. Simeda and A.A. Zaatout, *RSC Adv.*, **11**, 7851 (2021); https://doi.org/10.1039/D0RA08488C
11. G.Ö. Kayan and A. Kayan, *J. Polym. Environ.*, **29**, 3477 (2021); https://doi.org/10.1007/s10924-021-02154-x
12. S. Radoor, J. Karayil, A. Jayakumar, D. Nandi, J. Parameswaranpillai, J. Lee, J.M. Shivanna, R. Nithya and S. Siengchin, *J. Polym. Environ.*, **30**, 3279 (2022); https://doi.org/10.1007/s10924-022-02421-5
13. P. Huang, J. Liu, F. Wei, Y. Zhu, X. Wang, C. Cao and W. Song, *Mater. Chem. Front.*, **1**, 1550 (2017); https://doi.org/10.1039/C7QM00079K
14. M. Khorshidi, S. Asadpour, N. Sarmast and M. Dinari, *J. Mol. Liq.*, **348**, 118399 (2022); https://doi.org/10.1016/j.molliq.2021.118399
15. M. Daud, A. Hai, F. Banat, M.B. Wazir, M. Habib, G. Bharath and M.A. Al-Harthi, *J. Mol. Liq.*, **288**, 110989 (2019); https://doi.org/10.1016/j.molliq.2019.110989
16. L. Jafari Foruzin, Z. Rezvani and B. Habibi, *Appl. Clay Sci.*, **188**, 105511 (2020); https://doi.org/10.1016/j.clay.2020.105511
17. G. Rathee, N. Singh and R. Chandra, *ACS Omega*, **5**, 2368 (2020); https://doi.org/10.1021/acsomega.9b03785
18. T.R.R. Timóteo, C.G. Melo, L.J.A. Danda, L.C.P.B.B. Silva, D.A.F. Fontes, P.C.D. Silva, C.S.B. Aguilera, L.P. Siqueira, L.A. Rolim and P.J. Rolim Neto, *Appl. Clay Sci.*, **180**, 105197 (2019); https://doi.org/10.1016/j.clay.2019.105197
19. D. Bharali and R.C. Deka, *J. Environ. Chem. Eng.*, **5**, 2056 (2017); https://doi.org/10.1016/j.jece.2017.04.012
20. S.S. Ravuru, A. Jana and S. De, *J. Hazard. Mater.*, **373**, 791 (2019); https://doi.org/10.1016/j.jhazmat.2019.03.122
21. M.A. Iqbal, L. Sun and M. Fedel, *SN Appl. Sci.*, **1**, 1415 (2019); https://doi.org/10.1007/s42452-019-1474-4

22. Z. Wang, L. Zhang, P. Fang, L. Wang and W. Wang, *ACS Omega*, **5**, 21805 (2020); https://doi.org/10.1021/acsomega.0c02875
23. H. Lv, H. Rao, Z. Liu, Z. Zhou, Y. Zhao, H. Wei and Z. Chen, *J. Energy Storage*, **52B**, 104940 (2022); https://doi.org/10.1016/j.est.2022.104940
24. I. Langmuir, *J. Am. Chem. Soc.*, **40**, 1361 (1918); https://doi.org/10.1021/ja02242a004
25. H. Freundlich, *J. Phys. Chem.*, **57**, 385 (1906).
26. M.I. Temkin and V. Pyzhev, *Acta Physiochimica URSS*, **12**, 327 (1940).
27. M.K. Raman and G. Muthuraman, *Asian J. Chem.*, **31**, 1255 (2019); https://doi.org/10.14233/ajchem.2019.21772
28. S. Lagergren, *K. Sven. Vetensk. Akad. Handl.*, **24**, 1 (1898).
29. Y.S. Ho and G. Mckay, *Chem. Eng. J.*, **70**, 115 (1998); https://doi.org/10.1016/S0923-0467(98)00076-1
30. W.J. Weber and J.C. Morris, *J. Sanit. Eng. Div.*, **89**, 31 (1963).
31. J.R. Guarin, J.C. Moreno-Pirajan and L. Giraldo, *J. Chem.*, **2018**, 2124845 (2018); https://doi.org/10.1155/2018/2124845
32. J.M. Jabar, Y.A. Odusote, K.A. Alabi and I.B. Ahmed, *Appl. Water Sci.*, **10**, 136 (2020); https://doi.org/10.1007/s13201-020-01221-3
33. F.C. Wu, R.L. Tseng and R.S. Juang, *Chem. Eng. J.*, **153**, 1 (2009); https://doi.org/10.1016/j.cej.2009.04.042
34. F.C. Wu, R.L. Tseng and R.S. Juang, *Chem. Eng. J.*, **150**, 366 (2009); https://doi.org/10.1016/j.cej.2009.01.014
35. H.T.N. Thi, D.C. Nguyen, T.T. Nguyen, V.T. Tran, H.V. Nguyen, L.G. Bach, D.V.N. Vo, D.H. Nguyen, D.V. Thuan, S.T. Do and T.D. Nguyen, *Key Eng. Mater.*, **814**, 463 (2019); https://doi.org/10.4028/www.scientific.net/KEM.814.463
36. D. Maiti, S. Mukhopadhyay and P.S. Devi, *ACS Sustain. Chem. Eng.*, **5**, 11255 (2017); https://doi.org/10.1021/acssuschemeng.7b01684
37. K.L. Muedi, V. Masindi, J.P. Maree, N. Haneklaus and H.G. Brink, *Nanomaterials*, **12**, 776 (2022); https://doi.org/10.3390/nano12050776
38. A. Li, H. Deng, C. Ye and Y. Jiang, *ACS Omega*, **5**, 15152 (2020); https://doi.org/10.1021/acsomega.0c01092
39. B. Priyadarshini, T. Patra and T.R. Sahoo, *J. Magnes. Alloys*, **9**, 478 (2021); https://doi.org/10.1016/j.jma.2020.09.004
40. R. Lafi, K. Charradi, M.A. Djebbi, A.B. Haj Amara and A. Hafiane, *Adv. Powder Technol.*, **27**, 232 (2016); https://doi.org/10.1016/j.apt.2015.12.004
41. J. Li, H. Yu, X. Zhang, R. Zhu and L. Yan, *Front. Environ. Sci. Eng.*, **14**, 52 (2020); https://doi.org/10.1007/s11783-020-1229-x
42. H.A. Tabti, B. Medjahed, M. Boudinar, A. Kadeche, N. Bouchikhi, A. Ramdani, S. Taleb and M. Adjdir, *Res. Chem. Intermed.*, **48**, 2683 (2022); https://doi.org/10.1007/s11164-022-04722-9
43. S. Chilukoti and T. Thangavel, *Inorg. Chem. Commun.*, **100**, 107 (2019); https://doi.org/10.1016/j.inoche.2018.12.027
44. I.M. Ahmed and M.S. Gasser, *Appl. Surf. Sci.*, **259**, 650 (2012); https://doi.org/10.1016/j.apsusc.2012.07.092
45. T. Taher, R. Putra, N. Rahayu Palapa and A. Lesbani, *Chem. Phys. Lett.*, **777**, 138712 (2021); https://doi.org/10.1016/j.cplett.2021.138712
46. C. Suppaso, N. Pongkan, S. Intachai, M. Ogawa and N. Khaorapapong, *Appl. Surf. Sci.*, **213**, 106115 (2021); https://doi.org/10.1016/j.clay.2021.106115
47. P. Chakraborty and R. Nagarajan, *Appl. Surf. Sci.*, **118**, 308 (2015); https://doi.org/10.1016/j.clay.2015.10.011
48. J. Li, N. Zhang and D.H.L. Ng, *J. Mater. Chem. A.*, **3**, 21106 (2015); https://doi.org/10.1039/C5TA04497A